

## Article

# Utilization of Waste Marble and Bi<sub>2</sub>O<sub>3</sub>-NPs as a Sustainable Replacement for Lead Materials for Radiation Shielding Applications

Khalid Alsafi <sup>1,2</sup>, Mohamed A. El-Nahal <sup>3</sup> , Wafa M. Al-Saleh <sup>4,5</sup> , Haifa M. Almutairi <sup>6</sup>, Esraa H. Abdel-Gawad <sup>3</sup>  and Mohamed Elsafi <sup>7,\*</sup> 

- <sup>1</sup> Medical Physics Unit, Department of Radiology, Faculty of Medicine, King Abdulaziz University, Jeddah 21859, Saudi Arabia; kalsafi@kau.edu.sa
  - <sup>2</sup> Medical Physics Unit, Diagnostic Imaging Department, King Abdulaziz University Hospital, Jeddah 21859, Saudi Arabia
  - <sup>3</sup> Environmental Studies Department, Institute of Graduate Studies and Research, Alexandria University, Alexandria 21544, Egypt; igsr.nahalmoh@alexu.edu.eg (M.A.E.-N.); esraaabdelgawad@alexu.edu.eg (E.H.A.-G.)
  - <sup>4</sup> College of Science and Health Professions, King Saud Bin Abdulaziz University for Health Sciences, Hofuf 31982, Al-Ahsa, Saudi Arabia; salehw@ksau-hs.edu.sa
  - <sup>5</sup> King Abdullah International Medical Research Center, Hofuf 36428, Al-Ahsa, Saudi Arabia
  - <sup>6</sup> Department of Physics, Faculty of Sciences, Umm AL-Qura University, Mecca 24382, Saudi Arabia; hmutayri@uqu.edu.sa
  - <sup>7</sup> Physics Department, Faculty of Science, Alexandria University, Alexandria 21511, Egypt
- \* Correspondence: mohamedelsafi68@gmail.com

**Abstract:** In an attempt to reutilize marble waste, a new approach is presented in the current study to promote its use in the field of shielding against ionizing radiation. In this study, we aimed to develop a novel and sustainable/eco-friendly lead-free radiation shielding material by improving artificial marble (AM) produced from marble waste combined with polyester by reinforcing it with bismuth oxide (Bi<sub>2</sub>O<sub>3</sub>) nanoparticles. Six samples of AM samples doped with different concentrations (0%, 5%, 10%, 15%, 20%, and 25%) of Bi<sub>2</sub>O<sub>3</sub> nanoparticles were prepared. The linear attenuation coefficient (*LAC*) values were measured experimentally through the narrow beam method at different energies (0.0595 MeV, 0.6617 MeV, 1.1730 MeV, and 1.330 MeV) for all samples with various concentrations of Bi<sub>2</sub>O<sub>3</sub>. Radiological shielding parameters such as half value layer (*HVL*), tenth-value layer (*TVL*), and radiation shielding efficiency (*RSE*) were estimated and compared for all the different samples. The results prove that increasing the concentration of Bi<sub>2</sub>O<sub>3</sub> leads to the enhancement of the radiation shielding properties of the AM as a shielding material. It was observed that as the energy increases, the efficiency of the samples falls. High energy dependence was found when calculating the *HVL* and *TVL* values of the samples, which increased with increases in the energy of the incident photons. A comparison between the sample with the most efficient gamma radiation attenuation capability (AM-25%), concrete, and lead was conducted, and a discussion regarding their radiation shielding properties is presented herein. The results show that the AM-25% sample is superior to the ordinary concrete over all the studied energy ranges, as evidenced by its significantly lower *HVL*s. On the contrary, lead is superior to the AM-25% sample over all the studied energy ranges owing to its unbeatable density as a shielding material. Overall, this new type of artificial marble has the potential to be used as a radiation shielding material at low- to medium-gamma energy regions, specifically in medical imaging and radiation therapy.

**Keywords:** marble waste; waste management; artificial marble; polyester; ionizing radiation; radiation shielding; free-lead materials; nanoparticles; bismuth oxide



**Citation:** Alsafi, K.; El-Nahal, M.A.; Al-Saleh, W.M.; Almutairi, H.M.; Abdel-Gawad, E.H.; Elsafi, M. Utilization of Waste Marble and Bi<sub>2</sub>O<sub>3</sub>-NPs as a Sustainable Replacement for Lead Materials for Radiation Shielding Applications. *Ceramics* **2024**, *7*, 639–651. <https://doi.org/10.3390/ceramics7020042>

Academic Editor: Ashutosh Goel

Received: 20 February 2024

Revised: 24 April 2024

Accepted: 30 April 2024

Published: 7 May 2024



**Copyright:** © 2024 by the authors. Licensee MDPI, Basel, Switzerland. This article is an open access article distributed under the terms and conditions of the Creative Commons Attribution (CC BY) license (<https://creativecommons.org/licenses/by/4.0/>).

## 1. Introduction

The marble industry produces vast quantities of waste during the quarrying and subsequent processing of rocks [1]. By-product waste can be classified into three types of waste, fine powder waste (marble dust), coarse waste (various shapes and sizes of rock fragments), and slurry (mud) produced during the cutting process of marble slabs [1]. The disposal of marble waste is considered an economic and environmental problem [1]. Fine marble powders result in air and visual pollution. Moreover, marble slurry and residues could cause water pollution, soil pollution, and environmental deterioration through the air [2]. The reutilization of marble waste protects our environment from pollution and adds more economic value to the marble industry since more than 50% of marble is converted to waste after mining and processing. As marble slurry generated from processing units dries, it leaves a surface residue that pollutes the air, and due to rain, this waste could contaminate surface water [3,4].

At the same time, developing a variety of radiation shielding materials is necessary to match the increasing ionizing radiation applications in the medicine, energy, industry, agriculture, and research sectors [5]. Exposure to high doses of ionizing radiation could lead to huge risks to human health, and the use of shielding materials is considered the most effective approach for shielding against radiation [6–8].

Many previous studies have been conducted to investigate the possibility, efficiency, and feasibility of using marble waste to develop radiation shielding materials, mostly in the form of concrete [9–11], aiming to increase the attenuation of ionizing radiation by raising the density of concrete. Using marble waste as a partial replacement for some components of the concrete mix has been proven to increase gamma attenuation power, improve some mechanical and physical properties like compressive strength, and decrease the water permeability of concrete [12]. Moreover, marble waste has been added to other materials like clays, bricks, cement pastes, and polymers [11,13,14]. Focusing on polymers in particular, lately, they have become popular to use in inventing upgraded materials to shield against radiation. Polyester, polypyrrole, polyvinyl chloride, isophthalic resin, ethylene vinyl acetate, methyl vinyl silicone rubber, styrene-butadiene rubber, and polydimethylsiloxane are the most frequently used polymers including several additives for the innovation of adequate radiation shielding materials thanks to their durability, light weight, flexibility, and good mechanical properties [15]. Having the lowest shrinkage quality, outstanding resistance against chemical deterioration, shape stability, and greater compression, fatigue, and tensile strength, polyester polymers are the most favorable among all polymers, and their properties can be further improved by introducing different metal oxides [16–19].

Pioneering researchers have conducted extensive investigations of the radiation shielding properties of materials produced by combining marble waste with polyester resin. Elhemily, H. and her colleagues [20] investigated the effect of introducing different concentrations and sizes (micro and nano) of tungsten oxide ( $\text{WO}_3$ ) on the radiation shielding capabilities of crumbly waste marbles mixed with polyester. Their composites with higher  $\text{WO}_3$  concentrations had higher linear attenuation coefficient ( $LAC$ ) values. In terms of their results, the radiation shielding efficiency ( $RSE$ ) of waste marble + polyester +  $\text{WO}_3$  demonstrated that their marble composites absorb almost all incoming photons at low energies. Moreover, the effect of increasing the concentration of lead carbonate ( $\text{PbCO}_3$ ) and cadmium oxide ( $\text{CdO}$ ) contents on the physical properties and radiation attenuation factors of a newly developed radiation shielding absorber fabricated by Sayyed, M. and his team [21] was experimentally examined. The  $LAC$  values for all the marble compositions were highest at the lowest energy (0.06 MeV), while the  $LAC$  decreased with increasing energy. The highest  $LAC$  was found for Marb-3, with a composition of waste marble (50 wt%), polyester (25 wt%),  $\text{PbCO}_3$  (17.5 wt%), and  $\text{CdO}$  (7.5 wt%). They also studied the impact of the addition of  $\text{CdO}$  to substitute  $\text{PbCO}_3$ , and they found that the half-value layer ( $HVL$ ) decreases with increasing  $\text{CdO}$  content. On top of that, Almuqrin, A. and his fellow workers [22] have developed a new shielding material based on waste marble and polyester. It was made by the combination of polyester and fine waste marble, mixed along

with lead oxide (PbO) and bismuth oxide (Bi<sub>2</sub>O<sub>3</sub>). Their newly prepared shield's *HVL* and mean free path (*MFP*) exhibited that the sample PWPBi-10—composed of polyester (40 wt%), fine waste marble (30 wt%), PbO (20 wt%), and Bi<sub>2</sub>O<sub>3</sub> (10 wt%)—provides an excellent shielding capability compared to the other investigated polyester samples. The *MFP* behavior reveals that the ratio of PbO and Bi<sub>2</sub>O<sub>3</sub> on those novel polyesters has a direct effect on their radiation shielding characteristics. It is worth noting that the novel polyester sample, PWPBi-10, exhibited the lowest *MFP* value compared to the rest of the tested samples.

As a continuation of earlier efforts, the aim of the research presented herein was to develop a novel lead-free radiation shielding material by utilizing artificial marble (AM) produced from marble waste and polyester resin while reinforcing it with nanoscale Bi<sub>2</sub>O<sub>3</sub> particles. Bismuth is a heavy metal, and it has a higher atomic number than lead and a density close to lead, but it is not toxic to human beings and can be considered an eco-friendly chemical element, unlike lead, which has adverse harmful effects on the environment and humans during its production, usage, and disposal. Also, nano Bi<sub>2</sub>O<sub>3</sub> could enhance gamma attenuation and some physical properties of the designed material [23,24]. For the novel designed mixture, six samples of AM with nano-sized Bi<sub>2</sub>O<sub>3</sub> (as a filler) were prepared, and the radiation shielding properties of the fabricated composites (waste marble + polyester + nano-Bi<sub>2</sub>O<sub>3</sub>) were recorded. Experiments were conducted using a high-purity germanium detector (HPGe detector) and different radioactive point sources (<sup>241</sup>Am, <sup>137</sup>Cs-, and <sup>60</sup>Co). The linear attenuation coefficients (*LACs*) for the samples were determined experimentally at 0.06, 0.662, 1.173, and 1.333 MeV. Additional shielding parameters, such as half-value length (*HVL*), tenth-value length (*TVL*), and radiation shielding efficiency (*RSE*), were calculated for the novel designed marble formations.

## 2. Materials and Methods

### 2.1. Preparation

Artificial marble (AM) was prepared using polyester resin in liquid form, crumbly waste marble, calcium carbonate (CaCO<sub>3</sub>), and bismuth oxide (Bi<sub>2</sub>O<sub>3</sub>). Table 1 shows the characteristics of the liquid polyester resin used in this study. Waste marble (coarse marble) with an average diameter of 5 mm was collected from a marble factory. A fine powder of CaCO<sub>3</sub> was added to the mixture to improve the AM's texture and strength. Bi<sub>2</sub>O<sub>3</sub> nanoparticles, which were added to the AM to improve its capabilities to attenuate to the incident photons, were purchased from Nanotech company, Cairo, Egypt.

**Table 1.** Polyester resin characteristics.

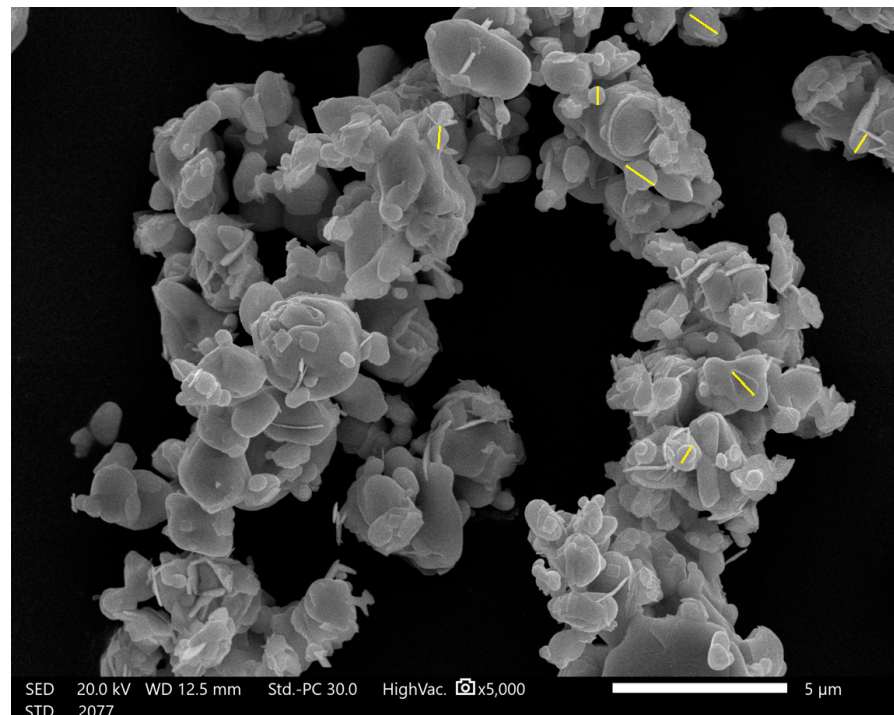
|                                 |      |
|---------------------------------|------|
| Density (g·cm <sup>-3</sup> )   | 1.25 |
| Yield Modulus (GPa)             | 2–4  |
| Compressive Strength (MPa)      | 140  |
| Tensile Strength (MPa)          | 55   |
| Tensile Elongation at Break (%) | 2    |

The polyester resin was gradually added to CaCO<sub>3</sub> with continuous stirring to make sure that the mixture was free of agglomeration; then, the required amount of waste marble was added with Bi<sub>2</sub>O<sub>3</sub> nanoparticles. The compound was stirred well, poured into molds, and left for 24 h until completely dry and hardened. The chemical composition, densities, and codes of the prepared AM samples are listed in Table 2. The density of the samples was measured practically using the mass per volume law, where the mass was measured using a 0.0001 digital balance, and the volume was measured by the ( $x \pi r^2$ ) formula, where  $x$  and  $r$  represent the thickness and the radius of a sample.

**Table 2.** Chemical compositions, densities, and the codes of the prepared samples.

| Code   | Chemical Composition wt (%) |                   |              |  | Density (g/cm <sup>3</sup> ) |
|--------|-----------------------------|-------------------|--------------|--|------------------------------|
|        | Polyester                   | CaCO <sub>3</sub> | Waste Marble | Bi <sub>2</sub> O <sub>3</sub> Nanoparticles |                              |
| AM-0%  | 25                          | 25                | 50           | 0  | 2.07                         |
| AM-5%  | 25                          | 25                | 50           | 5  | 2.13                         |
| AM-10% | 25                          | 25                | 50           | 10   | 2.19                         |
| AM-15% | 25                          | 25                | 50           | 15   | 2.25                         |
| AM-20% | 25                          | 25                | 50           | 20   | 2.32                         |
| AM-25% | 25                          | 25                | 50           | 25   | 2.39                         |

A Scanning Electron Microscope (SEM) (JEOL model, Japanese-made and available at the Faculty of Science, Alexandria University in Egypt) was used to photograph the Bi<sub>2</sub>O<sub>3</sub> powder nanoparticles before they were added to the marble formation to determine their average size. An SEM image of the Bi<sub>2</sub>O<sub>3</sub> powder nanoparticles is shown in Figure 1. From the SEM imaging, it was confirmed that the size of the used Bi<sub>2</sub>O<sub>3</sub> particles is less than 500 nm, with an average of 80 nm, and that the shape of the particles is spherical, as shown in the figure.

**Figure 1.** SEM image of Bi<sub>2</sub>O<sub>3</sub> nanoparticles.

## 2.2. Radiation Shielding Measurements

The attenuation of the prepared AM samples (waste marble + polyester + nano-Bi<sub>2</sub>O<sub>3</sub>) was determined experimentally using an HPGe detector and different point sources, including <sup>137</sup>Cs, <sup>60</sup>Co, and <sup>241</sup>Am (the mechanism for our measurements is illustrated in Figure 2). These radioactive sources were used because they emit photons of different energies, where the <sup>241</sup>Am source emits energy in the low range (0.060 MeV); this energy plays an important role in X-ray imaging, while <sup>60</sup>Co-60 (1.173 and 1.333 MeV) and <sup>137</sup>Cs (0.622 MeV) play an important role in medical, industrial, and agricultural applications, as well as food preservation applications, and therefore, they are dealt with continuously. Therefore, we focused on the energies that come out of them and how to reduce their effect and hazards. Within a certain time, the peaks related to the incoming energy photons emitted from the

source are formed. The area under these peaks can be calculated using Genie-2000 software, and the rate of this area (calculated area per measuring time) represents the intensity of the incoming photon. The intensity in the absence of an AM sample is represented by the initial intensity ( $I_0$ ), while by placing each AM sample between the detector and the point source, the calculated intensity is represented by the transmitted intensity ( $I$ ). From these values, the linear attenuation coefficient ( $LAC$ ) for a sample of a thickness ( $x$ ) can be calculated by the following equation [25,26]:

$$LAC = \frac{1}{x} \ln \frac{I_0}{I} \quad (1)$$

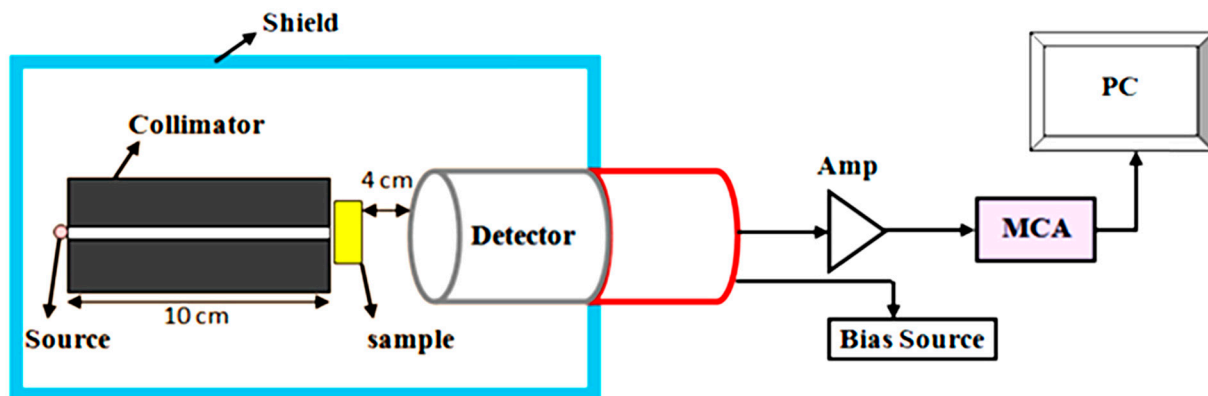


Figure 2. The experimental setup for measuring the attenuation coefficient.

The experimental results of the AM-microcomposites were compared with the results obtained from using Phy-x software [27], which is an easy-to-use online program for calculating parameters relevant to radiation attenuation and dosimetry. The other essential attenuator factors, such as the half-value length ( $HVL$ ), tenth-value length ( $TVL$ ), and radiation shielding efficiency ( $RSE$ ), for any AM sample can be expressed by the following equations:

$$HVL = \frac{\ln 2}{LAC} \quad (2)$$

$$TVL = \frac{\ln (10)}{LAC} \quad (3)$$

$$MFP = \frac{1}{LAC} \quad (4)$$

$$RSE\% = \left(1 - \frac{I}{I_0}\right) \times 100 \quad (5)$$

### 3. Results and Discussion

Some marble rocks have high radioactivity, and some have radioactivity values that are below the detection limit. To be environmentally safe, the radioactivity concentration of the used marble waste was determined, as this waste was collected from a factory in which three types of marble (Breshia, Galala, and Trista) were used. We conducted a gamma spectrometry analysis (high-purity germanium with a relative efficiency of 24% and resolution of 1.96 keV at 1.333 MeV). The results showed that the activity concentrations of the used marble waste were below the detection limits, as shown in Table 3. The largest concentration obtained for the Trista marble type belonged to the Rd-226 sample, with a concentration of  $23.69 \text{ Bq kg}^{-1}$ , which is a small concentration that does not affect human health, especially considering that the quantities used in sample preparation are not large.

**Table 3.** Marble-specific activities ( $\text{Bq kg}^{-1}$ ).

| Samples | Activity Concentrations of Studied Radionuclides |                 |                 |
|---------|--|-----------------|-----------------|
|         | $C_{\text{Ra}}$                                  | $C_{\text{Th}}$ | $C_{\text{K}}$  |
| Brescia | L.L.D  | $1.36 \pm 0.11$ | L.L.D           |
| Galala  | $13.68 \pm 5$                                    | $2.60 \pm 0.35$ | $4.90 \pm 1.45$ |
| Trista  | $23.69 \pm 2.8$                                  | $5.59 \pm 0.27$ | $5.27 \pm 0.51$ |

$C_{\text{Ra}}$ ,  $C_{\text{Th}}$ , and  $C_{\text{K}}$  represent the activity concentrations of  $^{226}\text{Ra}$ ,  $^{232}\text{Th}$ , and  $^{40}\text{K}$ , respectively, and L.L.D represents lower-level detectability (the uncertainties are quoted for a coverage factor  $k = 2$ ).

To evaluate the radiation shielding efficiency of the artificial marble (AM) samples (waste marble + polyester + nano- $\text{Bi}_2\text{O}_3$ ) enhanced by various concentrations of bismuth oxide ( $\text{Bi}_2\text{O}_3$ ) nanoparticles, the accuracy of the experimental results were confirmed through a comparison between theoretical *LAC* values from PHY-X and the experimental results of the AM samples prepared without nanoparticles of  $\text{Bi}_2\text{O}_3$  [28]. The PHY-X and experimental results, along with their relative deviations, are illustrated in Figure 3. The theoretical and experimental values of the linear attenuation coefficients (*LACs*) match well together, with relative deviations below 5%, as reported in Table 4.

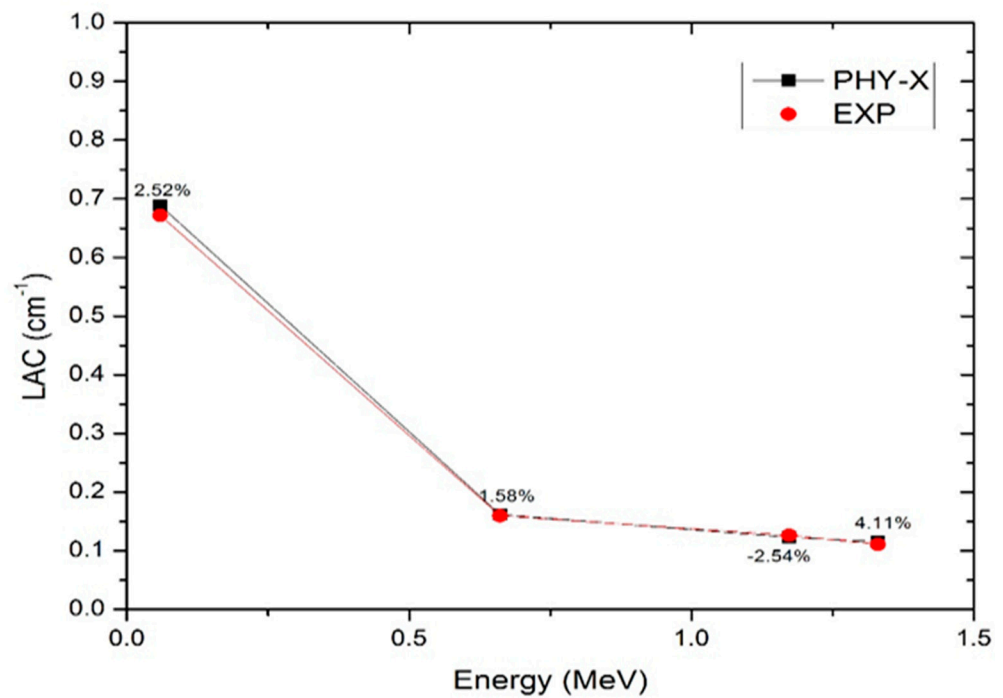


**Figure 3.** The experimental and theoretical *LACs* of the pure artificial sample and the relative deviations.

**Table 4.** The experimental and theoretical *LAC* values of the presented microcomposite AM (AM-0%).

| Code  | Energy, MeV | Phy-X | EXP               | DEV (%) |
|-------|-------------|-------|-------------------|---------|
| AM-0% | 0.060       | 0.689 | $0.672 \pm 0.009$ | 2.52    |
|       | 0.662       | 0.162 | $0.160 \pm 0.003$ | 1.58    |
|       | 1.173       | 0.123 | $0.126 \pm 0.005$ | -2.54   |
|       | 1.333       | 0.115 | $0.111 \pm 0.004$ | 4.11    |

Figure 4 demonstrates that the increase in *LACs* is proportional to the concentration of  $\text{Bi}_2\text{O}_3$  nanoparticles because  $\text{Bi}_2\text{O}_3$  is a heavy metal oxide (Bi atomic number = 83), so it can increase the probability of the photoelectric interaction of the incident gamma rays with the samples. It is worth mentioning that the *LACs* decrease with increasing photon energy for all  $\text{Bi}_2\text{O}_3$  nanoparticle concentrations because the Compton scattering and pair production interaction are most likely to happen at medium (0.661 MeV) and high (1.173 and 1.33 MeV) energies, and these interactions are less closely related to the atomic number [29]. Table 5 compares the *LAC* values against the  $\text{Bi}_2\text{O}_3$  nanoparticle concentrations for different energies.

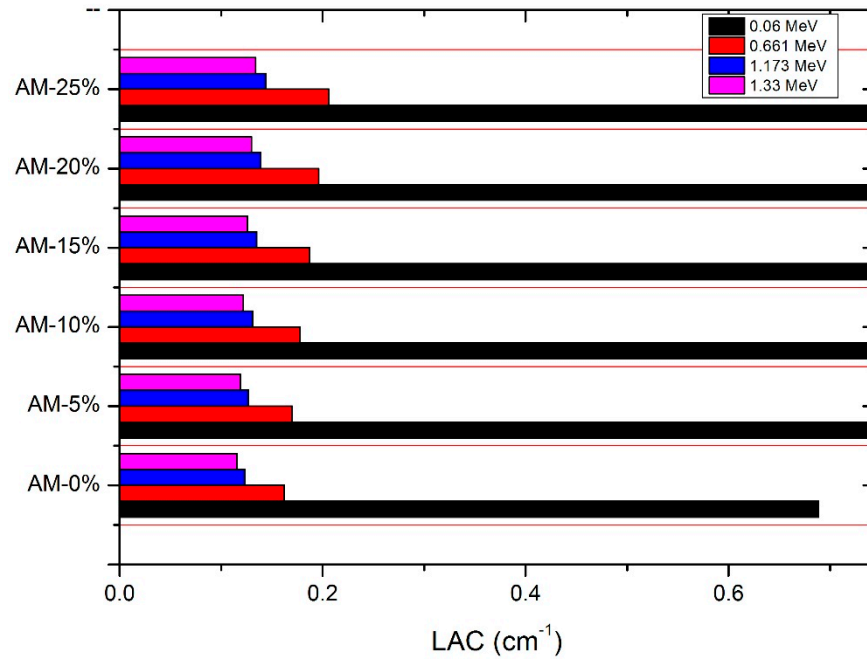


Figure 4. The *LACs* of the designed artificial marble samples.

Table 5. A comparison of the *LAC* values against the  $\text{Bi}_2\text{O}_3$  nanoparticle concentrations for different energies.

| Parameter                     | Energy, MeV | AM-5%             | AM-10%            | AM-15%            | AM-20%            | AM-25%            |
|-------------------------------|-------------|-------------------|-------------------|-------------------|-------------------|-------------------|
| <i>LAC</i> , $\text{cm}^{-1}$ | 0.060       | $1.178 \pm 0.005$ | $1.695 \pm 0.003$ | $2.242 \pm 0.003$ | $2.821 \pm 0.004$ | $3.436 \pm 0.004$ |
|                               | 0.662       | $0.170 \pm 0.007$ | $0.178 \pm 0.005$ | $0.187 \pm 0.004$ | $0.196 \pm 0.006$ | $0.206 \pm 0.004$ |
|                               | 1.173       | $0.127 \pm 0.002$ | $0.131 \pm 0.001$ | $0.135 \pm 0.005$ | $0.139 \pm 0.003$ | $0.144 \pm 0.002$ |
|                               | 1.333       | $0.119 \pm 0.009$ | $0.122 \pm 0.004$ | $0.126 \pm 0.002$ | $0.130 \pm 0.002$ | $0.134 \pm 0.005$ |

The half-value length (*HVL*) and tenth-value length (*TVL*) are related to the *LAC* of each sample. They decreased with an increase in the content of the nano-sized  $\text{Bi}_2\text{O}_3$  particles and increased as the photon energy was raised. The *HVLs* have their maxima at zero  $\text{Bi}_2\text{O}_3$  content (AM-0%), with the highest being a value of 6.0 cm at a photon energy of 1.33 MeV, while its minima is at the highest concentration of  $\text{Bi}_2\text{O}_3$  (AM-25%), with a value of 0.2 cm at a gamma energy value of 0.06 MeV. A similar behavior can be observed for the *TVLs*. (see Figures 5 and 6). Table 6 presents a comparison of the *HVL* and *TVL* values against the  $\text{Bi}_2\text{O}_3$  nanoparticle concentrations for different energies.

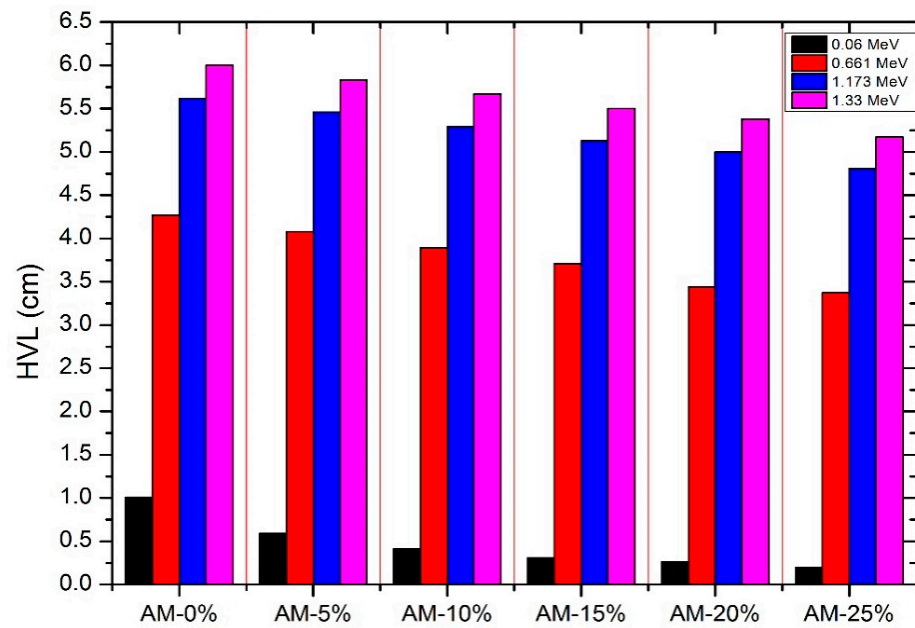


Figure 5. The HVLs of the designed artificial marble samples.

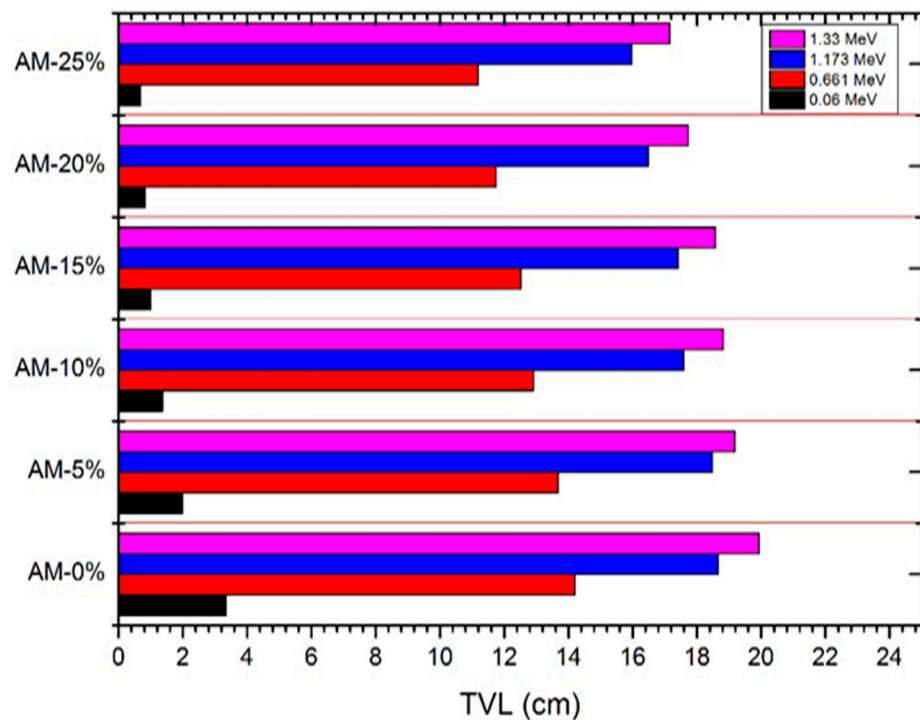


Figure 6. The TVLs of the designed artificial marble samples.

The most important factor is the radiation shielding efficiency (*RPE*). At a practical and operational thickness of 2 cm, it manifests the radiation shielding properties of the investigated samples. From Figure 7, it can be deduced that the AM-25% sample (25%  $\text{Bi}_2\text{O}_3$  NPs) had the maximum *RPE* over all the energy ranges, with approximately 100% radiation absorption efficiency at 0.06 MeV photon energy. When this energy range is exceeded, the efficiency is decreased to about 46.06% at a radiation energy of 0.661 MeV. The lowest *RPE* value for the samples with 25%  $\text{Bi}_2\text{O}_3$  NPs was 33.11% at 1.33 MeV. The *RSE* values at different thicknesses (2, 5, and 8 cm) are presented in Table 8.

**Table 6.** A comparison of the HVLs and TVLs against the Bi<sub>2</sub>O<sub>3</sub> nanoparticle concentrations for different energies.

| Parameter | Energy, MeV | AM-5%          | AM-10%         | AM-15%         | AM-20%         | AM-25%         |
|-----------|-------------|----------------|----------------|----------------|----------------|----------------|
| HVL, cm   | 0.060       | 0.588 ± 0.005  | 0.409 ± 0.002  | 0.309 ± 0.004  | 0.246 ± 0.007  | 0.202 ± 0.002  |
|           | 0.662       | 4.080 ± 0.002  | 3.892 ± 0.007  | 3.711 ± 0.005  | 3.537 ± 0.004  | 3.369 ± 0.004  |
|           | 1.173       | 5.459 ± 0.002  | 5.295 ± 0.004  | 5.132 ± 0.007  | 4.971 ± 0.002  | 4.810 ± 0.006  |
|           | 1.333       | 5.836 ± 0.005  | 5.669 ± 0.007  | 5.503 ± 0.006  | 5.337 ± 0.006  | 5.171 ± 0.005  |
| Parameter | Energy, MeV | AM-5%          | AM-10%         | AM-15%         | AM-20%         | AM-25%         |
| TVL, cm   | 0.060       | 1.954 ± 0.004  | 1.358 ± 0.006  | 1.027 ± 0.002  | 0.816 ± 0.003  | 0.670 ± 0.006  |
|           | 0.662       | 13.554 ± 0.005 | 12.929 ± 0.007 | 12.329 ± 0.002 | 11.750 ± 0.001 | 11.193 ± 0.003 |
|           | 1.173       | 18.134 ± 0.002 | 17.591 ± 0.003 | 17.050 ± 0.005 | 16.512 ± 0.004 | 15.977 ± 0.005 |
|           | 1.333       | 19.387 ± 0.002 | 18.833 ± 0.003 | 18.280 ± 0.002 | 17.728 ± 0.008 | 17.178 ± 0.006 |

The mean free path (*MFP*) is also related to the *LAC* of each sample. The *MFP* values decreased with an increase in the content of the nano-sized Bi<sub>2</sub>O<sub>3</sub> particles and increased as the photon energy was raised. The *MFP* was highest at zero Bi<sub>2</sub>O<sub>3</sub> content (AM-0%), with a value of 8.661 cm at a photon energy of 1.333 MeV, while the *MFP* was lowest at the highest concentration of Bi<sub>2</sub>O<sub>3</sub> (AM-25%), with a value of 0.291 cm at a gamma energy value of 0.060 MeV. A comparison of the *MFP* values against the Bi<sub>2</sub>O<sub>3</sub> nanoparticle concentrations for different energies is presented in Table 7.

**Table 7.** A comparison of the *MFP* values against the Bi<sub>2</sub>O<sub>3</sub> nanoparticle concentrations for different energies.

| Parameter | Energy, MeV | AM-5%         | AM-10%        | AM-15%        | AM-20%        | AM-25%        |
|-----------|-------------|---------------|---------------|---------------|---------------|---------------|
| HVL, cm   | 0.060       | 0.849 ± 0.004 | 0.590 ± 0.002 | 0.446 ± 0.005 | 0.354 ± 0.001 | 0.291 ± 0.002 |
|           | 0.662       | 5.886 ± 0.002 | 5.615 ± 0.003 | 5.354 ± 0.007 | 5.103 ± 0.004 | 4.861 ± 0.007 |
|           | 1.173       | 7.876 ± 0.001 | 7.639 ± 0.002 | 7.405 ± 0.004 | 7.171 ± 0.007 | 6.939 ± 0.004 |
|           | 1.333       | 8.420 ± 0.006 | 8.179 ± 0.007 | 7.939 ± 0.008 | 7.699 ± 0.003 | 7.460 ± 0.002 |

**Table 8.** The RSE values at different thicknesses (2, 5, and 8 cm) and different energies.

|               | Energy, MeV | AM-0%  | AM-5%  | AM-10%  | AM-15%  | AM-20%  | AM-25%  |
|---------------|-------------|--------|--------|---------|---------|---------|---------|
| RSE, % (2 cm) | 0.060       | 74.773 | 90.522 | 96.629  | 98.871  | 99.645  | 99.896  |
|               | 0.662       | 27.692 | 28.807 | 29.965  | 31.170  | 32.425  | 33.730  |
|               | 1.173       | 21.848 | 22.427 | 23.033  | 23.670  | 24.339  | 25.042  |
|               | 1.333       | 20.619 | 21.143 | 21.693  | 22.270  | 22.877  | 23.516  |
|               | Energy, MeV | AM-0%  | AM-5%  | AM-10%  | AM-15%  | AM-20%  | AM-25%  |
| RSE, % (5 cm) | 0.060       | 96.804 | 99.723 | 99.979  | 99.999  | 100.000 | 100.000 |
|               | 0.662       | 55.540 | 57.234 | 58.953  | 60.696  | 62.462  | 64.249  |
|               | 1.173       | 46.005 | 46.999 | 48.030  | 49.097  | 50.205  | 51.354  |
|               | 1.333       | 43.858 | 44.780 | 45.737  | 46.731  | 47.765  | 48.840  |
|               | Energy, MeV | AM-0%  | AM-5%  | AM-10%  | AM-15%  | AM-20%  | AM-25%  |
| RSE, % (8 cm) | 0.060       | 99.595 | 99.992 | 100.000 | 100.000 | 100.000 | 100.000 |
|               | 0.662       | 72.663 | 74.311 | 75.943  | 77.556  | 79.148  | 80.713  |
|               | 1.173       | 62.695 | 63.788 | 64.908  | 66.054  | 67.228  | 68.430  |
|               | 1.333       | 60.294 | 61.332 | 62.399  | 63.495  | 64.621  | 65.779  |

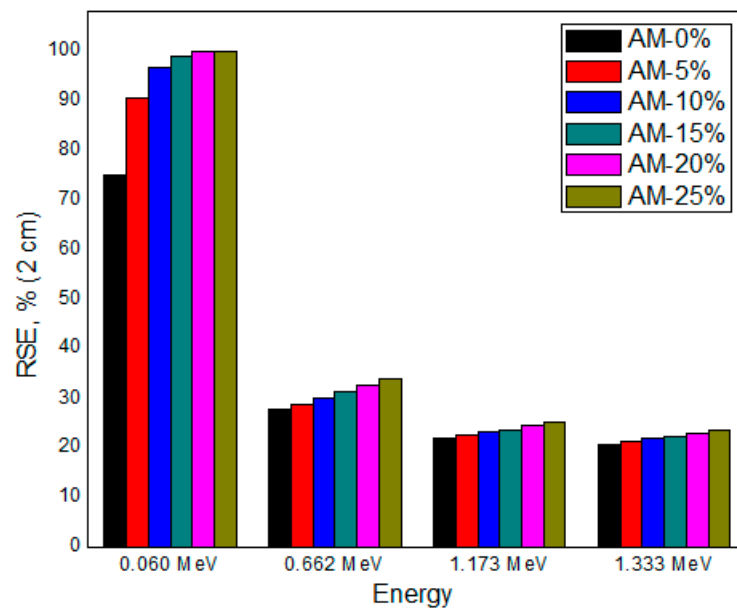


**Figure 7.** The *RPE* values of the designed artificial marble samples.

To determine whether the newly designed and manufactured samples of AM reinforced with  $\text{Bi}_2\text{O}_3$  NPs are practically efficient in terms of radiation attenuation, they were compared with the most commonly used building material (ordinary concrete) and the most efficient and commonly used radiation shielding material (lead). It was concluded that the AM sample with the highest concentration of 25% of  $\text{Bi}_2\text{O}_3$  NPs (AM-25%) has efficient gamma radiation attenuation capabilities, so a comparison between AM-25%, concrete, and lead regarding their radiation shielding properties was carried out. The *HVLs* will be the measure for this comparison (Figure 8). From the figure below, it can be observed that at 0.662 MeV, the thickness needed to attenuate or absorb most of the incoming radiation was nearly 30 cm for AM-25%, while for ordinary concrete, it was around 37 cm, as calculated based on Equations (1) and (5).

The results show that the AM-25% sample outperforms ordinary concrete over all the studied energy ranges, as evidenced by its significantly lower *HVLs* at the low energy range (0.059 MeV) due to the influenced of the atomic number-dependent photoelectric effect interaction over this energy region. The composition of AM-25% has Ca and Bi ( $Z = 20$  and  $Z = 83$ ) as the main elements, while ordinary concrete is predominantly composed of silica, i.e., Si ( $Z = 14$ ), which has a lower atomic number. On the contrary, lead outperforms AM-25% over all the studied energy ranges due to its higher density and atomic number, which makes its shielding performance unconquerable despite its environmental issues. After all, it can be settled that these designed AM samples are very efficient at low energy to medium (0.4 MeV to 0.661 MeV) gamma energy regions as radiation shielding materials. Hence, they could be used as convenient gamma radiation shielding materials in medical diagnosis X-rays (conventional X-ray and CT imaging) because the utilized energy range of medical X-ray imaging is from 0.01 MeV to 0.15 MeV [30].

Finally, the attenuation results of the current work were compared with related works, and as shown in tabulated form in Table 9. The data in the table show that the manufactured marble samples studied in this work provide suitable results as a shield against gamma rays, especially at low energies, as at 0.060 MeV, AM25% performs slightly better than AM-WO<sub>3</sub> and similar PWPBi-composites, while at higher energies, there are no significant differences.

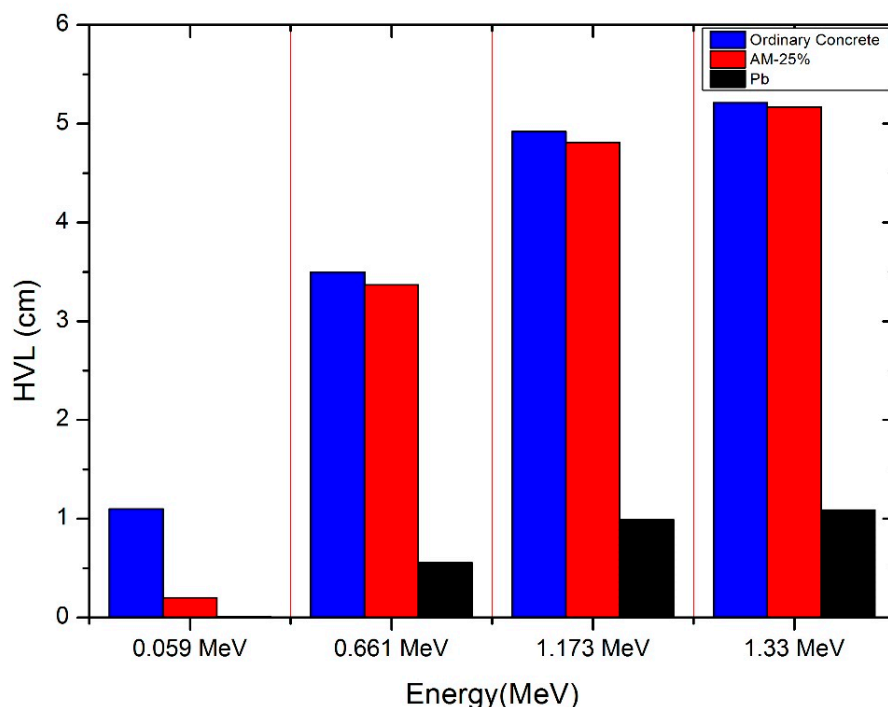


Figure 8. The HVLs of ordinary concrete, AM-25%, and lead.

Table 9. A comparison of the marbles from the present work with materials from other published works.

| Reference             | Sample Code | LAC, cm <sup>-1</sup> |           |           |           | TVL, cm   |           |           |           |
|-----------------------|-------------|-----------------------|-----------|-----------|-----------|-----------|-----------|-----------|-----------|
|                       |             | 0.060 MeV             | 0.662 MeV | 1.173 MeV | 1.333 MeV | 0.060 MeV | 0.662 MeV | 1.173 MeV | 1.333 MeV |
| AM-WO3 [21]           | S1          | 2.862                 | 0.191     | 0.139     | 0.129     | 0.805     | 12.049    | 16.577    | 17.794    |
|                       | S2          | 2.872                 | 0.197     | 0.140     | 0.130     | 0.802     | 11.694    | 16.459    | 17.699    |
|                       | S3          | 2.886                 | 0.200     | 0.142     | 0.132     | 0.798     | 11.524    | 16.238    | 17.457    |
|                       | S4          | 2.991                 | 0.211     | 0.144     | 0.134     | 0.770     | 10.908    | 16.035    | 17.248    |
| PWPBi-composites [22] | PWPBi-5     | 3.505                 | 0.190     | 0.131     | 0.122     | 0.657     | 12.111    | 17.530    | 18.874    |
|                       | PWPBi-10    | 3.506                 | 0.190     | 0.131     | 0.122     | 0.657     | 12.114    | 17.537    | 18.882    |
|                       | PWPBi-20    | 3.510                 | 0.190     | 0.131     | 0.122     | 0.656     | 12.116    | 17.542    | 18.887    |
|                       | PWPBi-30    | 3.512                 | 0.190     | 0.131     | 0.122     | 0.656     | 12.123    | 17.555    | 18.902    |
| Present Work          | AM-10%      | 1.695                 | 0.178     | 0.131     | 0.122     | 1.358     | 12.929    | 17.591    | 18.833    |
|                       | AM-15%      | 2.242                 | 0.187     | 0.135     | 0.126     | 1.027     | 12.329    | 17.050    | 18.280    |
|                       | AM-20%      | 2.821                 | 0.196     | 0.139     | 0.130     | 0.816     | 11.750    | 16.512    | 17.728    |
|                       | AM-25%      | 3.436                 | 0.206     | 0.144     | 0.134     | 0.670     | 11.193    | 15.977    | 17.178    |

4. Conclusions

The present study was performed to estimate the radiation shielding characteristics of innovative fabricated artificial marble (AM) composites made of waste marble with polyester resin embedded with nano-sized bismuth oxide (Bi<sub>2</sub>O<sub>3</sub>) in different concentrations. An experimental approach was employed to find out the linear attenuation coefficient (LAC) for each of the prepared AM samples and then calculate other shielding parameters using the determined LAC values. The LAC values obtained from the pure AM (without nanoparticles of Bi<sub>2</sub>O<sub>3</sub>) using the Phy-X software were consistent with the experimental

values measured using an HPGe (high-purity germanium) detector, which is considered an indication of the accuracy of the results. The uniform distribution of the Bi<sub>2</sub>O<sub>3</sub> nanoparticles, through the AM samples' matrices, was proven to enhance the attenuation capabilities of the samples. Increasing the Bi<sub>2</sub>O<sub>3</sub> content enhanced the shielding performance of the AM composites in terms of the LAC. The proportionality relation between the LACs and the concentration of Bi<sub>2</sub>O<sub>3</sub> nanoparticles in the composites was highly distinguished in the low-energy radiation zone; on the other hand, it was not as noticeable in the high-energy zone. Regarding the other shielding parameters of the composites under study, such as the half-value layer (HVL) and tenth-value layer (TVL), they decreased with increasing Bi<sub>2</sub>O<sub>3</sub> NP concentrations. To comprehensively understand more of the characteristics of waste marble composites with potential as shielding materials against ionizing radiation, future studies should investigate incorporating additional types of polymers with the waste marble, such as epoxy resin, polydimethylsiloxane, polyvinyl chloride, etc.

**Author Contributions:** Conceptualization, M.E.; methodology, M.A.E.-N.; software, E.H.A.-G.; validation, W.M.A.-S., H.M.A. and K.A.; formal analysis, M.A.E.-N.; investigation, M.E.; resources, W.M.A.-S.; data curation, K.A.; writing—original draft preparation, M.A.E.-N.; writing—review and editing, M.E.; visualization, E.H.A.-G.; supervision, M.E.; project administration, H.M.A.; funding acquisition, W.M.A.-S. All authors have read and agreed to the published version of the manuscript.

**Funding:** This research received no external funding.

**Institutional Review Board Statement:** Not applicable.

**Informed Consent Statement:** Not applicable.

**Data Availability Statement:** The original contributions presented in the study are included in the article, further inquiries can be directed to the corresponding author.

**Conflicts of Interest:** The authors declare no conflict of interest.

## References

1. Singh, M.; Choudhary, K.; Srivastava, A.; Sangwan, K.S.; Bhunia, D. A study on environmental and economic impacts of using waste marble powder in concrete. *J. Build. Eng.* **2017**, *13*, 87–95. [CrossRef]
2. Sharma, N.; Singh Thakur, M.; Goel, P.; Sihag, P. A review: Sustainable compressive strength properties of concrete mix with replacement by marble powder. *J. Achiev. Mater. Manuf. Eng.* **2020**, *98*. [CrossRef]
3. Pappu, A.; Saxena, M.; Asolekar, S.R. Waste to wealth-cross sector waste recycling opportunity and challenges. *Can. J. Environ. Constr. Civ. Eng.* **2011**, *2*, 14–23.
4. Singh, M.; Srivastava, A.; Bhunia, D. An investigation on effect of partial replacement of cement by waste marble slurry. *Constr. Build. Mater.* **2017**, *134*, 471–488. [CrossRef]
5. Reilly, D.; Ensslin, N.; Smith, H., Jr.; Kreiner, S. Passive Nondestructive Assay of Nuclear Materials; Nuclear Regulatory Commission, Washington, DC, USA. 1991. Available online: <https://www.nrc.gov/docs/ML0914/ML091470585.pdf> (accessed on 1 March 2020).
6. Pentreath, R. Radiation protection of people and the environment: Developing a common approach. *J. Radiol. Prot.* **2002**, *22*, 45. [CrossRef] [PubMed]
7. Alabsy, M.T.; Alzahrani, J.S.; Sayyed, M.I.; Abbas, M.I.; Tishkevich, D.I.; El-Khatib, A.M.; Elsafi, M. Gamma-Ray Attenuation and Exposure Buildup Factor of Novel Polymers in Shielding Using Geant4 Simulation. *Materials* **2021**, *14*, 5051. [CrossRef] [PubMed]
8. Ron, E. Cancer risks from medical radiation. *Health Phys.* **2003**, *85*, 47–59. [CrossRef]
9. El-Nahal, M.A.; Elsafi, M.; Sayyed, M.; Khandaker, M.U.; Osman, H.; Elesawy, B.H.; Saleh, I.H.; Abbas, M.I. Understanding the effect of introducing micro- and nanoparticle bismuth oxide (Bi<sub>2</sub>O<sub>3</sub>) on the gamma ray shielding performance of novel concrete. *Materials* **2021**, *14*, 6487. [CrossRef]
10. Gur, A.; Artig, B.; Cakir, T. Photon attenuation properties of concretes containing magnetite and limonite ores. *Physicochem. Probl. Miner. Process.* **2017**, *53*, 184–191.
11. Martínez-Barrera, G.; Menchaca-Campos, C.; Gencil, O. Polyester polymer concrete: Effect of the marble particle sizes and high gamma radiation doses. *Constr. Build. Mater.* **2013**, *41*, 204–208. [CrossRef]
12. Ghani, A.; Ali, Z.; Khan, F.A.; Shah, S.R.; Khan, S.W.; Rashid, M. Experimental study on the behavior of waste marble powder as partial replacement of sand in concrete. *SN Appl. Sci.* **2020**, *2*, 1554. [CrossRef]
13. AYGUN, Z.; Aygün, M.; Yarbaşı, N. A study on radiation shielding potentials of green and red clayey soils in Turkey reinforced with marble dust and waste tire. *J. New Results Sci.* **2021**, *10*, 46–59. [CrossRef]

14. Obaid, S.S.; Sayyed, M.; Gaikwad, D.; Pawar, P.P. Attenuation coefficients and exposure buildup factor of some rocks for gamma ray shielding applications. *Radiat. Phys. Chem.* **2018**, *148*, 86–94. [[CrossRef](#)]
15. Hamisu, A.; Khiter, O.; Al-Zhrani, S.; Haridh, W.S.B.; Al-Hadeethi, Y.; Sayeed, M.; Tijani, S. The use of nanomaterial polymeric materials as ionizing radiation shields. *Radiat. Phys. Chem.* **2023**, *216*, 111448. [[CrossRef](#)]
16. Yasmin, S.; Almousa, N.; Abualsayed, M.I.; Elsafi, M. Grafting of heavy metal oxides onto pure polyester for the interest of enhancing radiation shielding performance. *Radiochim. Acta* **2023**, *111*, 495–502. [[CrossRef](#)]
17. Sayyed, M.I. Radiation shielding characterization of a Yb:CaTeX glass system as a function of TeO<sub>2</sub> concentration. *Opt. Quantum Electron.* **2024**, *56*, 333. [[CrossRef](#)]
18. Alasali, H.J.; Sayyed, M.I. Studies of gamma radiation attenuation properties of silica based commercial glasses utilized in Jordanian dwellings. *Opt. Quantum Electron.* **2024**, *56*, 391. [[CrossRef](#)]
19. Nabil, I.M.; El-Samrah, M.G.; Omar, A.; Tawfic, A.F.; El Sayed, A.F. Experimental, analytical, and simulation studies of modified concrete mix for radiation shielding in a mixed radiation field. *Sci. Rep.* **2023**, *13*, 17637. [[CrossRef](#)]
20. Hemily, H.M.; Saleh, I.; Ghataas, Z.; Abdel-Halim, A.; Hisam, R.; Shah, A.; Sayyed, M.; Yasmin, S.; Elsafi, M. Radiation shielding enhancement of polyester adding artificial marble materials and WO<sub>3</sub> nanoparticles. *Sustainability* **2022**, *14*, 13355. [[CrossRef](#)]
21. Sayyed, M.; Almurayshid, M.; Almasoud, F.I.; Alyahyawi, A.R.; Yasmin, S.; Elsafi, M. Developed a new radiation shielding absorber composed of waste marble, polyester, PbCO<sub>3</sub>, and CdO to reduce waste marble considering environmental safety. *Materials* **2022**, *15*, 8371. [[CrossRef](#)] [[PubMed](#)]
22. Almuqrin, A.H.; Yasmin, S.; Abualsayed, M.I.; Elsafi, M. An experimental investigation into the radiation-shielding performance of newly developed polyester containing recycled waste marble and bismuth oxide. *Appl. Rheol.* **2023**, *33*, 20220153. [[CrossRef](#)]
23. Sikora, P.; El-Khayatt, A.M.; Saudi, H.; Chung, S.-Y.; Stephan, D.; Abd Elrahman, M. Evaluation of the effects of bismuth oxide (Bi<sub>2</sub>O<sub>3</sub>) micro and nanoparticles on the mechanical, microstructural and  $\gamma$ -ray/neutron shielding properties of Portland cement pastes. *Constr. Build. Mater.* **2021**, *284*, 122758. [[CrossRef](#)]
24. Mhareb, M.H.A.; Alajerami, Y.S.M.; Sayyed, M.I.; Dwaikat, N.; Alqahtani, M.; Alshahri, F.; Saleh, N.; Alonizan, N.; Ghrib, T.; Al-Dhafar, S.I. Radiation shielding, structural, physical, and optical properties for a series of borosilicate glass. *J. Non-Cryst. Solids* **2020**, *550*, 120360. [[CrossRef](#)]
25. Ahmed, S.N. *Physics and Engineering of Radiation Detection*; Academic Press: Cambridge, MA, USA, 2007.
26. Nikjoo, H.; Uehara, S.; Emfietzoglou, D. *Interaction of Radiation with Matter*; CRC Press: Boca Raton, FL, USA, 2012.
27. Şakar, E.; Özpölat, Ö.F.; Alım, B.; Sayyed, M.I.; Kurudirek, M. Phy-X/PSD: Development of a user friendly online software for calculation of parameters relevant to radiation shielding and dosimetry. *Radiat. Phys. Chem.* **2020**, *166*, 108496. [[CrossRef](#)]
28. Alfryyan, N.; Alrowaili, Z.A.; Alomairy, S.; Nabil, I.M.; Al-Buriahi, M.S. Radiation Attenuation Properties of Zinc-Borosilicate Glasses Containing Al<sub>2</sub>O<sub>3</sub> and Gd<sub>2</sub>O<sub>3</sub>. *Silicon* **2023**, *15*, 8031–8043. [[CrossRef](#)]
29. Hubbell, J.H.; Seltzer, S.M. *Tables of X-ray Mass Attenuation Coefficients and Mass Energy-Absorption Coefficients 1 keV to 20 MeV for Elements Z = 1 to 92 and 48 Additional Substances of Dosimetric Interest*; National Inst. of Standards and Technology-PL: Gaithersburg, MD, USA, 1995.
30. Chen, G.-H.; Zambelli, J.; Bevins, N.; Qi, Z.; Li, K. X-ray phase sensitive imaging methods: Basic physical principles and potential medical applications. *Curr. Med. Imaging* **2010**, *6*, 90–99. [[CrossRef](#)]

**Disclaimer/Publisher’s Note:** The statements, opinions and data contained in all publications are solely those of the individual author(s) and contributor(s) and not of MDPI and/or the editor(s). MDPI and/or the editor(s) disclaim responsibility for any injury to people or property resulting from any ideas, methods, instructions or products referred to in the content.